Bioorganic Chemistry 54 (2014) 21–30

Contents lists available at ScienceDirect

Bioorganic Chemistry

journal homepage: www.elsevier.com/locate/bioorg

Molecular design and synthesis of 1,4-disubstituted piperazines as α_1-adrenergic receptor blockers

Dalal A. Abou El-Ella [a,*], Mohammed M. Hussein [b], Rabah A.T. Serya [a], Rana M. Abdel Naby [c], Ahmed M. Al-Abd [d], Dalia O. Saleh [d], Wafaa I. El-Eraky [d], Khaled A.M. Abouzid [a,*]

[a] Department of Pharmaceutical Chemistry, Faculty of Pharmacy, Ain Shams University, Abbasia 11566, Cairo, Egypt
[b] Department of Pharmaceutical Chemistry, Faculty of Pharmacy, Cairo University, Kasr El Aini 11562, Cairo, Egypt
[c] Department of Pharmaceutical Chemistry, Misr University for Science and Technology, Al-Motamayez, 6Th October, Egypt
[d] Department of Pharmacology, Medical Division, National Research Center, Dokki, Cairo, Egypt

ARTICLE INFO

Article history:
Received 25 October 2013
Available online 24 March 2014

Keywords:
Phenylpiperazines
Pyridothienopyrimidine
α_1-Adrenoreceptors blockers

ABSTRACT

A new series of 4,5,6,7-tetrahydrothieno[2,3-c]pyridine-3-carboxylic acid amide and 3,5,6,8-tetrahydropyrido[4′,3′:4,5]thieno[2,3-d]pyrimidin-4-one derivatives were designed, synthesized, their binding and functional properties as α_1-adrenoreceptors blockers were evaluated. A new validated α_1-adrenoreceptor blocker pharmacophore model (hypothesis) was generated using Discovery Studio 2.5. The compare-fit study for the designed molecules with the generated hypothesis was fulfilled and several compounds showed significant high fit values. Compounds ***IVa–c, VIIa–d, VIIIa–c, Xa–c, XIa–d*** have shown blocking activity ranging from 46.73% up to 94.74% compared to 99.17% for prazosin.

1. Introduction

Elevated blood pressure is a common disorder affecting high proportion of the community which may amounts up to 15% or more. Many of these individuals have no apparent signs which may lead to congestive heart failure, myocardial infarction, renal and even cerebrovascular damages. When dealt with early, the incidence of these morbidity and mortality may be decreased. Thus, the need for selective and safe antihypertensive drug became an important research point. By studying different classes of antihypertensive drugs, the α_1-adrenergic receptors (ARs) antagonists emerged as promising effective class with fewer side effects. The α1-adrenergic subtypes are members of the G-protein-coupled receptor (GPCR) superfamily. At least three distinct α_1-receptor subtypes have been reported on the basis of both pharmacology and molecular biology [1–7]. The GPCRs are integral membrane proteins and contain seven hydrophobic domains which are believed to be arranged in seven membrane spanning helices [7–9]. These helices are responsible for passing signals across the cell membrane after interaction with their ligand on the extracellular side. The binding of the ligand elicits a response felt by the G-protein on the intracellular side. The activated G-protein then sets a second messenger system in train. Different GPCRs recognize different ligands. For adrenergic receptors, the activating ligands are norepinephrine and epinephrine. Adrenoreceptors (AR) are classified into α-AR and β-AR [7]. α-ARs play a pivotal role in the regulation of a variety of physiological processes, particularly within the cardiovascular system and are divided into two main subtypes α1- and α2-ARs [2,8]. The α1 and α2-ARs are located in the vascular smooth muscle cell membrane, and upon stimulation by an appropriate agonist, mediate vasoconstriction. The simultaneous occurrence of both receptor subtypes on vascular smooth muscles indicate that α1 and α2-ARs could contribute to the maintenance of peripheral arterial tone and may play an important role in resistance seen in hypertension. α1-ARs modulate intercellular biochemical processes in response to changes in extracellular concentrations of the neurotransmitter norepinephrine and the circulating hormone epinephrine [9–11]. The α_1-adrenergic receptor subtypes (α_1A-, α_1B-, α_1D) are the prime mediators of smooth muscle contraction and hypertrophic growth, but their characterization in both binding and function have lagged the other adrenergic family members. The α_1A-ARs are the predominant receptor subtypes, causing vasoconstriction in many vascular beds, including the following arteries: mammary, mesenteric, splenic, hepatic, omental, renal, pulmonary, and epicardial coronary. It is also the predominant subtype in the vena cava and the saphenous and pulmonary veins. Together with the α_1B receptor subtype, it promotes cardiac growth and structure. The α_1B receptor subtype

* Corresponding authors.
E-mail addresses: dalal999@hotmail.com, dalal@pharm.asu.edu.eg (D.A. Abou El-Ella), abouzid@yahoo.com, khaled.abouzid@pharm.asu.edu.eg (K.A.M. Abouzid).

http://dx.doi.org/10.1016/j.bioorg.2014.03.005
0045-2068/

is the most abundant type in the heart, whereas the α_1D receptor subtype is the predominant receptor, causing vasoconstriction in the aorta [3]. Studies using young prehypertensive and adult spontaneously hypertensive rats as well as knockout mice suggest that vascular α_1D-adrenoceptors are involved in the genesis/maintenance of hypertension [26]. Compounds acting as antagonists at various post-junctional α1A-ARs are frequently used in the therapy of high blood pressure, most common drug are prazosin (***1***) [7,12], doxazosin (***2***) [6] and terazosin (***3***) [9]. They cause arterial and venous vasodilatation and consequently lower total peripheral resistance, lower arterial blood pressure, and decrease platelet aggregation. Also, they may be useful in the treatment of benign prostatic hyperplasia (BPH), lower urinary tract symptoms (LUTS), and cardiac arrhythmia [1–5]**.** But the available subtype-selective drugs such as BMY-7378 [6,12] and WAY-100635 (***5***) [10] are only moderately selective as native tissues can express all the three subtypes. Thus, the aim in this research is to develop more subtype selective antagonists with higher efficacy, minimum side effects, and better patient compliance.

In order to design such ligands, structural information on the receptor subtypes, especially their binding sites, would be invaluable. There is, however, no X-ray structure available for any GPCRs. Many GPCR transmembrane domains have been modeled on the basis of the known structure of bacteriorhodopsin, but these models are only qualitative in nature and are still under development [7–9].

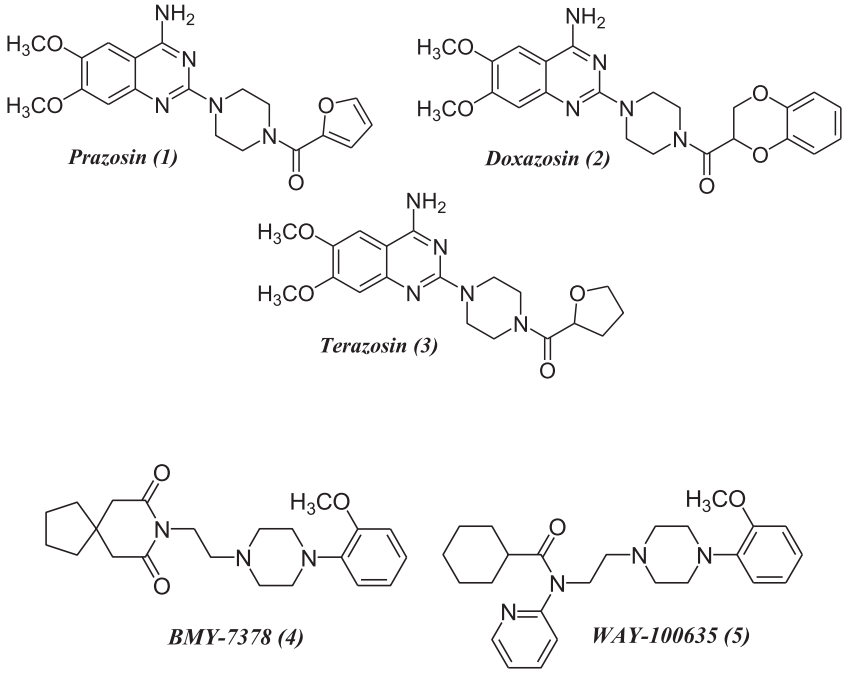

The most recent models elaborated using radioligand binding data of selective α_1-ARs antagonists and computer aided methods with catalyst have been proposed by Bremner et al. [6] and Barbaro et al. [7]. Barbaro's model, especially useful for phenylpiperazine derivatives had postulated five pharmacophore features [2,7]: a positive ionizable atom (PI), three hydrophobic regions (HY1–HY3), and a hydrogen bond acceptor (HBA). As 2-substituted phenylpiperazines derivatives, possess a positive ionizable nitrogen atom and an *ortho*-substituted phenyl ring corresponding to PI (***A***) and both HY1 and HY2 (***B***), respectively. These compounds also contain an additional hydrophobic moiety (ending the heterocyclic fragment) and a carbonyl group, which are corresponding to the HY3 and HBA features, respectively (***C***). Additionally, they possess an alkyl spacer between piperazine nitrogen and nitrogen placed close to carbonyl oxygen (HBA) at a chain or at heterocyclic rings. The alkyl spacer may be 2–7 carbons in length and may additionally be substituted with alkyl or hydroxyl moieties (Fig. 1) [8,9].

Based on the previously reported SAR, the target compounds (**IVa–c**, **VIa–d**, **VIIIa–c**, **Xa–c**, and **XIa–d**) were designed according to the following bioisosteric modification carried on reference compounds REC15/2739 (***6***) [6] and RN17 (***7***) [12] (Figs. 2 and 3). The influence of these bioisosteric modifications on their α_1-ARs affinity will be studied.

2. Results and discussion

2.1. Molecular modeling study

Molecular modeling studies were used to design a selective α_1A antagonists using pharmacophore modeling.

Pharmacophore modeling method has been widely used as a key tool of computer aided drug design in the lead discovery and optimization and also, to rationalize the relationship between the structural features and pharmacological activity. Molecular modeling simulation studies were performed by running the "common feature pharmacophore model" protocol in Discovery Studio 2.5 software and the generated pharmacophore model (hypothesis) for α1A-ARs antagonists was validated and used for virtual screening of the designed compounds that were proposed through SAR manipulation [2,6,7]. Lead compounds used to generate common feature pharmacophore are listed in (Table 1). The generated α_1A-AR antagonist hypotheses were subjected to simulation compare/fit studies (using the best-fit algorithmic method) with the conformational model of the proposed training set compounds to predict their α_1A-AR antagonist activities. The simulated fitting values of the best-fitted conformer may be a guide for prioritizing relative affinities of these compounds with the receptor. Consequently, the fit values between the reference drug prazosin (***1***) which is reported to posses high α_1A antagonistic activity [7,12], ***IVa–c***, ***VIa–d***, ***VIIIa–c***, ***Xa–c***, ***XIa–d***, and the α_1A-AR antagonist hypothesis were calculated separately.

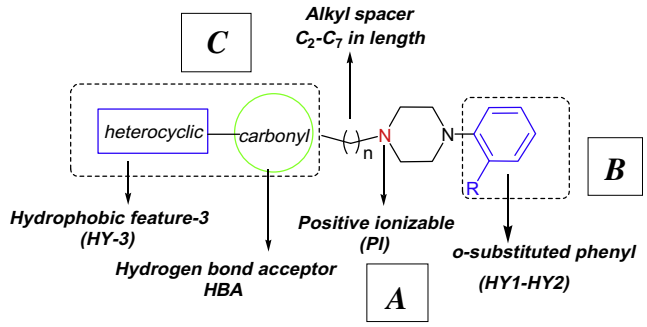

Fig. 1. SAR of α1-ARs antagonists.

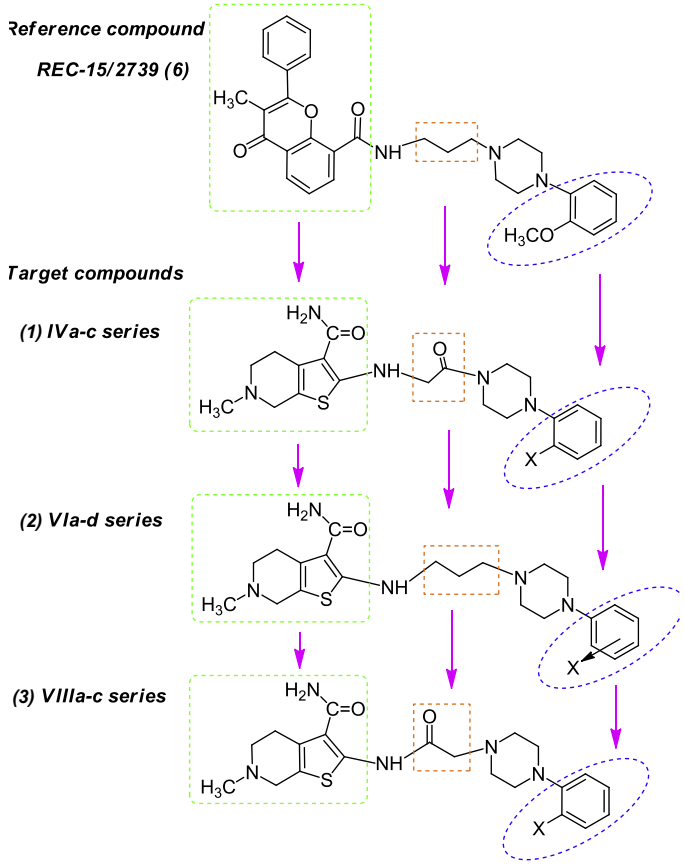

Fig. 2. The design of the target compounds IVa–c, VIa–d, and VIIIa–c by bioisosteric modification of the reference compound REC 15/2739 (6). The green dots represent the heteroaromatic moiety with carbonyl group (HY-3, HBA, respectively), the red dots represent the linker, and the blue dots represent the aryl group (HY-1, HY-2).

Table 1 shows of the results of the best fitting value of the best-fitted conformer of leads used to generate this hypothesis.

The training set used above are reported to have more potent antagonistic activity at α1A-AR over other subtypes [6,7] which might support the idea that the generated hypothesis will be more selective for α1A-AR antagonists. The common feature hypotheses generation gave 10 hypotheses. The assessment of the generated α_1-ARs antagonists hypotheses revealed that hypothesis ranking number 4 (Fig. 4) was proved to be the ideal one rather than the other generated hypothesis numbers. This was because hypothesis number 4 has more matched simulation data with experimental biological activity.

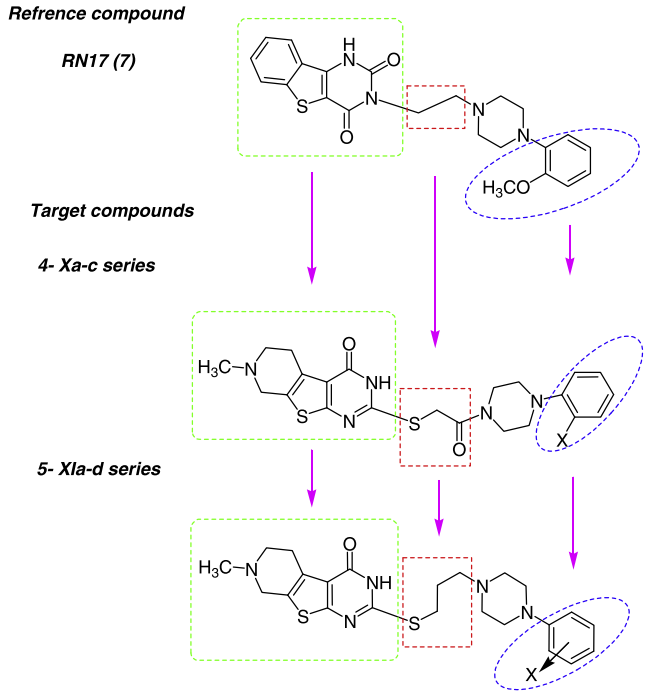

Fig. 3. The design of the target compounds Xa–d and XIa–d by bioisosteric modification of the reference compound RN17 (7). The dots colors are described in the legend of Fig. 2.

Table 1
Lead compounds used as training set in creating α_1A-ARs hypothesis.

Lead	Fitting values	Lead	Fitting values
Prazosin [7,12] (1)	3.83	SNAP-8719 [6,8]	1.02
BMY-7378 [6,12]	3.60	Terazosin [9]	3.22
WAY-100635 [10]	4.26	NAN-190 [7,11]	4.99
Abanoquil [6]	2.39	KMD-3213 [6,7]	3.54
REC-15/2739 [6]	4.20	RN17 [12]	3.56
Cyclazosin [6,10]	4.01	REC-15/2615 [6]	3.21
5-Me-urapidil [10]	3.90	WB4101 [6]	3.34
Benzoxathion [6]	4.26	Amiodarone [8]	2.06
A131701 [6]	2.63	SGB-1534 [7]	4.06
Tamsulosin [11]	1.33	Cdm-12 [7,8]	3.10

2.1.1. Validation of the generated pharmacophore model

The generated hypothesis encompassed five features namely; positive ionizable (PI), hydrogen bonding acceptor (HBA), and three hydrophobic features (HY1, HY2, and HY3) (Fig. 4), which was consistent with the reported literature [6,7].

*2.1.1.1. Mapping of prazosin (**1**) to the generated pharmacophore model.* This hypothesis showed full mapping of all of its five features with the lead structure of the Prazosin (Fig. 5).

2.1.1.2. Validation through mapping of certain reported active α_1A-AR antagonists (test set). Further validation included testing a reported highly selective α_1A-ARs antagonists [6,7] with the generated hypothesis and the simulation fit values showed good mapping with high fit values which validate the efficiency of our hypothesis as shown in (Table 2).

*2.1.2. Mapping of the target compounds **IVa–c**, **VIa–d**, **VIIIa–c**, **Xa–c**, and **XIa–d***

The newly designed molecules were subjected to molecular modeling study through ligand-pharmacophore mapping,

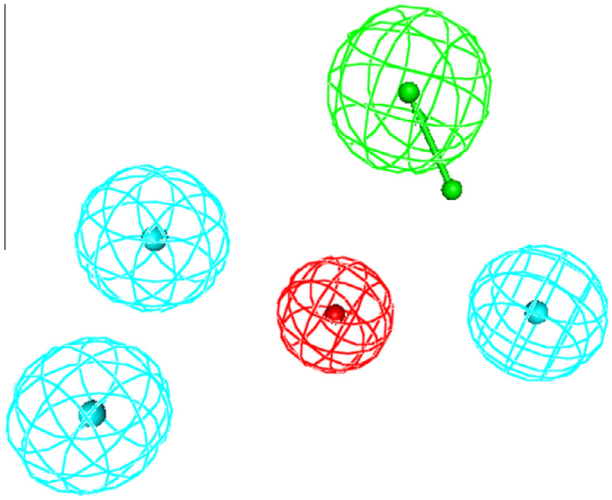

Fig. 4. Pharmacophore model of selective α1A-ARs antagonists generated by discovery studio 2.5. Pharmacophoric features are color coded: cyan for hydrophobic regions (HY1-3), green for hydrogen bond acceptor (HBA), and red for positive ionizable feature (PI).

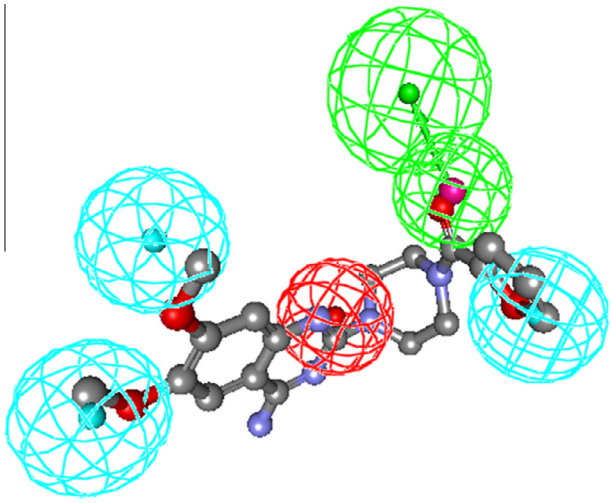

Fig. 5. Mapping of a1A-AR antagonist hypothesis and prazosin. The two o-methoxy groups of quinazoline moiety occupied both HY1 and HY2 (blue sphere) and the quinazoline N1 atom is located inside the positive ionizable feature PI (red sphere). The oxygen of the carbonyl group attached to piperazine overlapped HBA (green sphere), while the furan ring matched YH3 (blue sphere). The sphere colors are described in the legend of Fig. 4.

calculating the fitting value and comparing them to that of the reference compound. The results of the simulation study are summarized in (Table 3). The results of such simulation studies have revealed that most of the designed compounds would be promising active hit molecules.

The highest score compounds **IVb**, **VIIIb** and **XIb** mapping to the newly generated pharmacophore is illustrated in (Fig. 6).

2.1.3. Structure activity relationship of the investigated compounds

(1) The substitution on the phenyl ring of the arylpiperazine is crucial element for the α1-ARs blocking activity. As in the **IXa–d** series, there was a decrease in the activity by changing the substitution on the phenyl ring in the following order o-methoxy (94.74%) □ m-chloro (86.46%) □ unsubstituted (77.93%) □ o-flouro (65.68%). The same was observed in the **VIIIa–c** series; where compound **VIIIb** showed the highest activity among this series (78.27%) compared to 46.37% for the unsubstituted **VIIIa**. Also, in **VIa–c** series, o-methoxy has great effect on the activity where compound **VIb** showed 76.76% blocking activity compared to 69.93% for the m-chloro substituted **VId**. Unexpectedly in **Va–c** series, **Vc** with o-flouro substitution showed 88.88% blocking activity compared to o-methoxy **Vb** (81.15%). Thus the presence of a methoxy group at the ortho position seems optimum for the activity.

(2) The length of the alkyl spacer between N1 of the phenyl piperazine and the thienopyrimidine or thienopyridines rings is considered important for the α1-ARs blocking activity. A gradual decrease in the activity was observed by lengthening the spacer in the 6-methyl-4,5,6,7-tetrahydrothieno[2,3-c]pyridine-3-carboxylic acid amide analogs **Va–c**, **VIa–d**, and **VIIa–c**. Where the highest activity was

Table 2
Mapping of the test set (selective α_1A-AR antagonists) to the generated pharmacophore model.

Lead	Fitting value
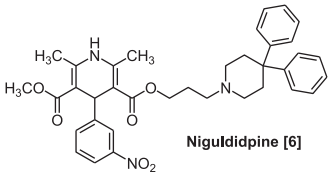 Niguldidpine [6]	4.71
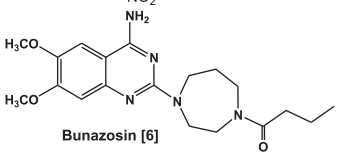 Bunazosin [6]	4.84
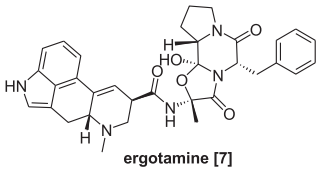 ergotamine [7]	4.15
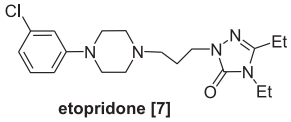 etopridone [7]	4.65

Table 3
Fitting and relative energy values of the best-fitted conformers of compounds IVa–c, VIa–d, VIIIa–c, Xa–c, XIa–d through mapping onto the pharmacophore model of the a_1-AR antagonist.

Test compounds	Fit values	Relative energy kcal/mol
IVa	4.69	56.8
IVb	4.93	51.27
IVc	***4.72***	44.98
VIa	1.68	37.38
VIb	4.81	7725
VIc	2.02	38.60
VId	***4.81***	38.69
VIIIa	1.80	36.60
VIIIb	***4.89***	196.53
VIIIc	1.90	16.40
Xa	4.49	77.50
Xb	4.56	23.18
Xc	4.54	46.56
XIa	4.57	19.90
XIb	***4.88***	13.25
XIc	4.58	32.38
XId	***4.73***	14.13

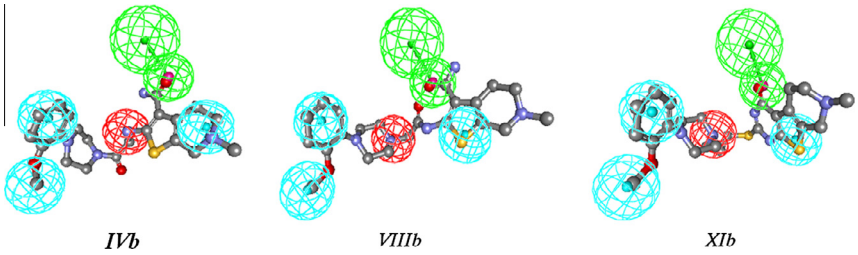

Fig. 6. Mapping of a1-AR antagonist hypothesis and compounds IVb, VIIIb, and XIb (fit value = 4.93, 4.89, and 4.88 respectively). o-Methoxyphenyl attached to piperazine moiety occupied both HY1 and HY2 (blue spheres) and the piperazinyl N-1 atom is located inside the positive ionizable feature PI (red sphere). The carbonyl oxygen of tetrahydropyridothienopyrimidine system overlapped HBA (green sphere), while its thiophene ring matched HY3 (blue sphere).

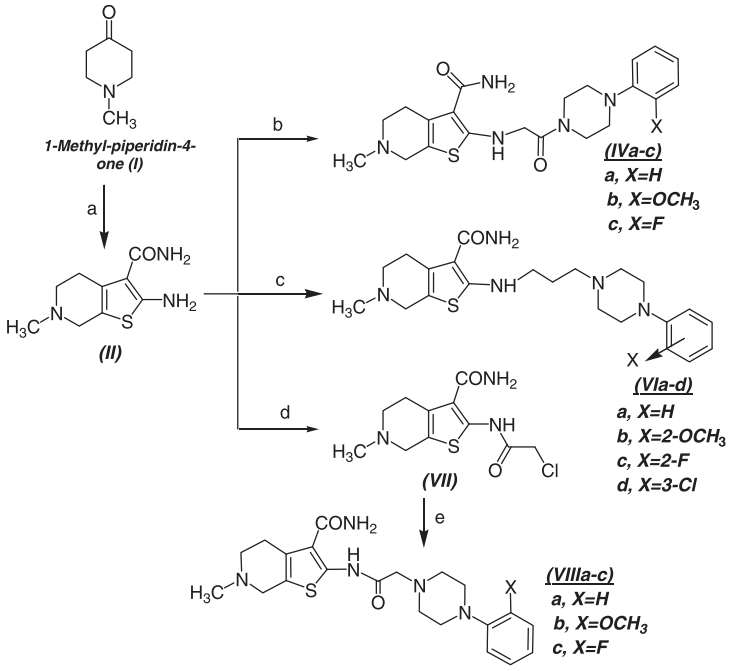

Scheme 1. Synthesis of target compounds IVa–c, VIa–d, VIIIa–c.

found in **Va–c** series compound **Vc** (88.88%), **Vb** (81.15%) characterized by two-carbon alkyl chain (2-oxo-ethyl-amino). For 5,6,7,8-tetrahydropyrido[4′,3′:4,5]-thieno[2,3-d]-pyrimidin-4(3H)-one analogs the opposite occur; changing the linker from 2carbon-chain (2-oxo-ethylamino-thio) in **VIIIa–c** series to propyl saturated chain in **IXa–d** series showed increase in the α1-ARs blocking activity, where compound **IXb** possesses 94.74% blocking activity compared to 78.27% for compound **VIIIb**. This may be contributed to placing the important features at good spacial distances that allowed good fitting with receptor.

(3) The thienopyrimidine and thienopyridine rings both have good effect on the activity as they fit in the third hydrophobic (HY-3) pocket in the receptor. By comparing the 6-methyl-4,5,6,7-tetrahydrothieno[2,3-c]pyridine-3-carboxylic acid amide and 5,6,7,8-tetrahydropyrido [4′,3′:4,5]-thieno[2,3-d]-pyrimidin-4(3H)-one analogs, it was obvious that they have comparable activities.

2.2. Chemistry

In Scheme 1, the *o*-amino amide (***II***) was prepared by the method reported by Gewald et al. [13] using 1-methyl-piperidin-4-one (***I***) as the starting reagent and 2-cyanoacetamide [14]; this o-amino amide (***II***) was N-alkylated in dry acetone and anhydrous K_2CO_3 with1-(2-chloroacetyl)-4-(2-substitutedphenyl)piperazines (***IIIa–c***) prepared as reported by Bourdais [15] to give the target compounds ***IVa–c*** [16–18]. Compounds ***VIa–d*** were prepared in the same manner as compounds ***IVa–c*** by alkylating o-amino amide (***II***) with 1-(2-substitutedphenyl)-4-(3-chloropropyl)-piperazines (***Va–c***) prepared in situ as hydrochloride salt for compounds ***VIa–c*** [15] or with the commercially available 1-(3-chlorophenyl)-4-(3-chloropropyl)-piperazine·2HCl for compound ***VId c*** [16–18]. Compounds ***VIIIa–c*** was prepared by refluxing compound (***VII***) with commercially available 2-substituted-phenylpiperazines in DMF and anhydrous K_2CO_3 [16,19].

In Scheme 2, the o-amino amide (***II***) was cyclized into compound (***IX***) [20,21] using CS_2 in NaOH; this key intermediate (***IX***) was furthe alkylated with phenylpiperazine derivatives (***IIIa–c***), (***Va–c***) or the commercially available 1-(3-chlorophenyl)-4-(3-chloropropyl)-piperazine·2HCl in ethanolic KOH [22,23] to give compounds ***Xa–c***, ***XIa–d,*** respectively. All the proposed structures were confirmed by Elemental Analysis, IR, and ^{1}H NMR data.

2.3. Biological evaluation

2.3.1. In vivo vasodilatation activity (functional bioassay)

Based on the fitting values obtained from Discovery studio, the active hits with best fitting values such as ***IVb***, ***IVc***, ***VIb***, ***VId***, ***VIIIb***, ***Xa–c*** and ***XIa–d*** were subjected to functional bioassay to evaluate

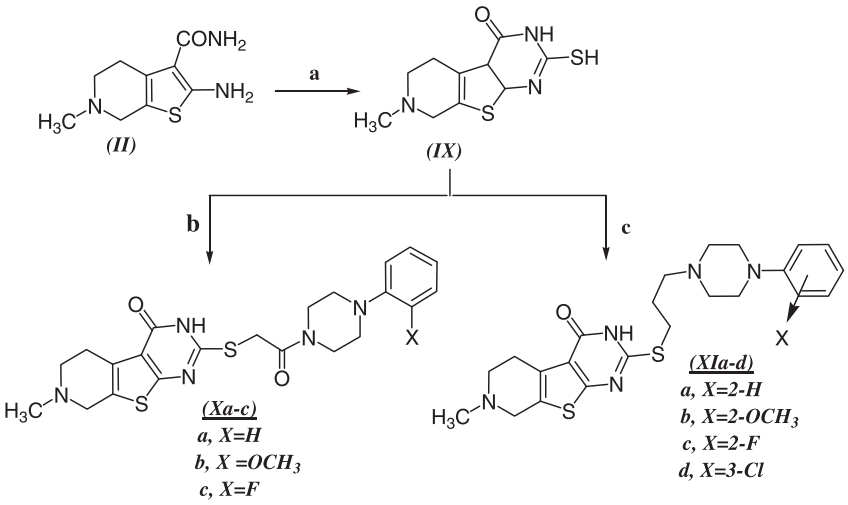

Scheme 2. Synthesis of target compounds Xa–c and XIa–d.

Table 4
Change in pre-treated aortic muscle tension after NE exposure. Change in tension is expressed as average muscle tone over duration of 1–2 min of recording.

	Induced change in aortic muscle tension (%)	Calculated α_1-ARs blocking activity (%)
Control (norepinephrine)	*100*	–
Prazosin (1)	*0.83*	*99.17*
IVb	*18.85*	***81.15***
IVc	*11.12*	***88.88***
VIb	*23.24*	*76.76*
VId	*30.07*	*69.93*
VIIIb	*29.45*	*70.55*
Xb	*21.73*	*78.27*
Xc	*28.53*	*71.47*
Xa	*53.63*	*46.37*
XIb	*5.26*	***94.74***
XId	*13.54*	***86.46***
XIa	*22.07*	*77.93*
XIc	*34.32*	*65.68*

their α_1-adrenoreceptors antagonistic activity, according to the standard procedure [24]. The antagonistic activity was assessed by the inhibition of the norepinephrine (NE)-induced contraction on isolated rat aorta tissues which predominantly express the α_1D-AR subtype which mediate vasoconstriction in rat aorta [2,25] and using prazosin (***1***) as the reference drug. Stimulation of α_1D-AR subtype is known to cause blood vessels contraction and control blood pressure.

Prazosin (***1***) completely abolished norepinephrine induced aortic contraction (B, 0.83%). Compounds ***IVc***, ***XIb,*** and ***XId*** showed the most potent α_1-blocking activity by inhibiting aortic tension to 11.1%, 5.3% and 13.5% its norepinephrine contracted tone (Table 4). Compounds ***IVb***, ***VIb***, ***VId***, ***Xb***, ***Xc***, ***XIa***, ***XIc,*** and ***VIIIb*** showed potentially strong α_1-blocking activity by decreasing the aortic tension to 18.9–34.3% of norepinephrine contracted aortic tension (Table 4). Only compounds ***Xa*** showed mild α_1-blocking activity by decreasing the aortic tension to 53.6% (Table 4).

2.3.2. Aortic ring tension recording

The change in pre-treated aortic muscle tension after nor epinephrine exposure was recorded (Table 4). This change in tension is expressed as average muscle tone over duration of 1–2 min of recording.

3. Conclusion

Novel series of 4,5,6,7-tetrahydrothieno[2,3-c]pyridine-3-carboxylic acid amide and 3,5,6,8-tetrahydropyrido[4′,3′:4,5]-thieno[2,3-d]pyrimidin-4-one derivatives were designed and synthesized. These 2 series were characterized by variable linker chain and substituents on the phenylpiperazine ring. The molecular modeling study helped to clarify molecular requirements for the design of high selective α_1-adrenergic ligands. The compounds that gave good fitting values through the pharmacophoric model were tested for their a_1-ARs antagonistic activity on isolated thoracic rat aorta. The tested compounds ***IVb***, ***IVc***, ***VIb***, ***Xb***, ***XIa***, ***XIb***, and ***XId*** showed comparable activity to prazosin (***1***) as reference standard and the results were matched with their high fitting values (Table 3). Some structural features have been proven to markedly affect the affinity to α_1-ARs blocking activity. In particular, the addition of *o*-methoxyphenyl on piperazine ring and presence of propyl spacer led to the best α_1-ARs affinity profile (high fitting value = 4.88; Fig. 6) and the highest α_1-ARs blocking activity (94.74% aortic ring inhibition) as in compound ***XIb***.

4. Experimental

4.1. Molecular modeling study

In this work, the pharmacophore hypothesis was produced using Accelrys Discovery Studio 2.5 in the computer drug design lab in Pharmaceutical Chemistry Department, Faculty of pharmacy, Ain Shams University. The set of conformational models of each structure of the lead compounds (Table 1) was performed and was used to generate the common feature hypotheses. The ideal hypothesis encompassed five features; positive ionizable nitrogen, three hydrophobic pockets and a hydrogen bond acceptor group.

4.1.1. Generation of the pharmacophore model for α_1-ARs antagonists

(1) The training set for the development of the pharmacophore has been chosen according to the catalyst guidelines and loaded into discovery studio.
(2) Generate hypothesis from this set using Protocol/Pharmacophore/Common Feature Pharmacophore Generation.
(3) Catalyst produces 10 hypotheses and Hypo5 is the best simulated pharmacophore hypothesis in this study, characterized by the highest cost difference, lowest error cost and

lowest root mean-square divergence and has the best correlation coefficient. All 10 hypotheses have the same features: one positive ionizable, one hydrogen-bond donor, one aromatic ring, and one hydrophobic group.

*4.1.2. Mapping of the test compounds (**IVa–c**, **VIa–d**, **VIIIa–c**, **Xa–c**, and **XIa–d**)*

1. The structures of the test set of the target and tetrahydrothienopyridines pyridothienopyrimidines were built using the Discovery Studio software.
2. Their conformational models were generated in the energy range of 20 kcal/mol above the estimated global energy minimum to ensure conformational diversity.
3. The fitting of the tested compounds was performed using ligand pharmacophore mapping protocol. The best fit option has been selected which manipulate conformers of each compound to find, when possible, different mapping modes of the ligand within the model. Mappings for all the test compounds to the hypothesis were visualized.

4.2. Chemistry

Melting points were determined by open capillary method using Electro thermal capillary melting point apparatus 9100 and were uncorrected. FT-IR spectra were recorded on a Shimadzu IR Affinity-1 Spectrophotometer, using KBr discs and measured by $\tilde{V}$, cm^{-1}. ^1H NMR spectra were recorded in δ scale given in ppm, performed on a JEOL ECA 300, 500 MHz spectrometer using $CDCl_3$ or DMSO as stated, using TMS as internal standard at National center for research and Cairo University. Mass spectra were performed on Shimadzu Qp-2010 plus (70 eV) spectrometer at Cairo University. Elemental analysis was performed at Azhar University. Progress of the reactions was monitored by TLC using pre-coated aluminum sheets silica gel ALUGRAM® SIL GLUV254 and was visualized under Vilber Lourmat UV lamp at 254 nm.

Compound II was prepared adopting the reported method [13,14] as follows:

*4.2.1. 2-Amino-6-methyl-4,5,6,7-tetrahydrothieno[2,3-c]pyridine-3-carboxylic acid amide (**II**)*

To a mixture of N-methylpiperdine-4-one (1.92 g, 0.0177 mol) and sulfur (0.62 g, 0.0195 mol) in (25 mL) absolute ethanol, cyanoacetamide (1.83 g, 0.0195 mol) was added, followed by slow addition of morpholine (2.5 mL). The reaction was heated at 40–50 °C for18 h, after which an equivalent amount of water was added and the mixture was refrigerated. The separated product was filtered, dried, and crystallized from ethanol/water mixture. **Yield:** 69%, found m.p.: 188–190 °C; reported m.p.:190 °C [14], IR (KBr, cm^{-1}): 3255–3410 (2 NH_2 stretching), 1674 (C=O).

*4.2.2. 2-(2-Chloroacetylamino)-6-methyl-4,5,6,7-tetrahydrothieno [2,3-c]pyridine-3-carboxylic acid amide (**VII**)*

A solution of **II** (2.11 g, 0.0100 mol) and sodium acetate (0.82 g) in DMF (17 mL) was kept in ice bath and chloroacetyl chloride (1.12 mL, 0.0100 mol) was added dropwise. The reaction was stirred at 20 °C for 3 h, and then poured into crushed ice. The separated solid was filtered, dried and crystallized from absolute ethanol. **Yield:** 59%; m.p.: 256–263 °C; FT-IR ($\tilde{V}$ max, cm^{-1}): 1724 (C=O); MS (*m/z*: M^+: 286, M+2: 288); ^1H NMR (300 MHz, $CDCl_3$): $\delta = 4.58$ (O=C—$\underline{CH_2}$—Cl).

*4.2.3. 2-Mercapto-7-methyl-3,5,6,8-tetrahydropyrido[4′,3′:4,5]thieno[2,3-d]pyrimidin-4-one (**IX**)*

A solution of **I** (2.11 g, 0.0100 mol) and NaOH (0.43 g, 0.0100 mol) in 10 mL ethanol/water mixture (5:1) was stirred for 30 min. CS_2 (0.90 mL, 0.0110 mol) was then added and stirring was continued for 20 h on cold. The reaction was diluted with an equivalent amount of water and acetic acid was added dropwise to render the medium slightly acidic. The solid formed was filtered, dried and crystallized from absolute ethanol. **Yield:** 95%; m.p.: 290–292 °C; FT-IR ($\tilde{V}$ max, cm^{-1}): 3506 cm^{-1} (NH, 2° amine).

*4.2.4. 2-Chloro-1-[4-(2-substitutedphenyl)-piperazin-1-yl]-ethanone derivatives (**IIIa–c**)*

Prepared according to the general procedure reported [15].

4.2.4.1. General procedure. To a solution of the corresponding arylpiperazines (0.0100 mol) in benzene (20 mL) and 2.5 mL 20% NaOH, chloroacetyl chloride (1.13 g, 0.0100 mol) was added dropwise with stirring at 0 °C. After complete addition, stirring was continued for 3 h at 0–10 °C. The benzene layer was washed with water and dried over anhydrous $MgSO_4$. The solvent was evaporated under vacuum leaving a solid material, which was collected, washed with ether and crystallized from n-hexane–benzene mixture, as reported [15].

*4.2.4.2. 2-Chloro-1-[4-(2-substituted-phenyl)-piperazin-1-yl]-ethanone (**IIIa**).* **Yield:** 59%; found m.p.: 76 °C, reported m.p.: 75 °C [15].

*4.2.4.3. 2-Chloro-1-[4-(2-substitutedphenyl)-piperazin-1-yl]-ethanone (**IIIb**).* **Yield:** 70%; found m.p.: 100 °C, reported m.p.: 100 °C [15].

*4.2.4.4. 2-Chloro-1-[4-(2-substitutedphenyl)-piperazin-1-yl]-ethanone (**IIIc**).* **Yield:** 49%; found m.p.: 112–114 °C, reported m.p.: 115 °C [15].

*4.2.4.5. 1-(2-Substitutedphenyl)-4-(3-chloropropyl)-piperazine. Dihydrochloride derivatives (**Va–c**).*

4.2.4.5.1. General procedures. A solution of the appropriate arylpiperazine (0.1000 mol), 1-bromo-3-chloropropane (18.9 mL, 0.1200 mol) and anhydrous K_2CO_3 (16.65 g, 0.1200 mol) in dry DMF (100 mL) was stirred at 20 °C for 24 h, after which it was filtered. To the filtrate, ethanolic HCl and diethyl ether was added portionwise till complete precipitation of the dihydrochloride derivatives. The solid was filtered and washed with ether to give compounds **Va–c** as reported [15].

*4.2.4.6. 1-(3-Chloropropyl)-4-phenylpiperazine.dihydrochloride (**Va**).* **Yield:** 75%; found m.p.: 160 °C, reported m.p. 160 °C [15].

*4.2.4.7. 1-(3-Chloropropyl)-4-(2-methoxyphenyl)piperazine. dihydrochloride (**Vb**).* **Yield:** 70%; found m.p.: 118–120 °C, reported m.p.: 120 °C [15].

*4.2.4.8. 1-(3-Chloropropyl)-4-(2-fluorophenyl)piperazine. dihydrochloride (**Vc**).* **Yield:** 49%; found m.p.: 165 °C, reported m.p.: 165 °C [15].

*4.2.5. 2-{2-[4-(2-Substitutedphenyl)piperazin-1-yl]-2-oxo-ethylamino}-6-methyl-4,5,7-tetrahydrothieno[2,3-c]pyridine-3-carboxylic acid amide derivatives (**IVa–c**)*

4.2.5.1. General procedures. The titled compounds were prepared by refluxing a mixture of **II** (2.11 g, 0.0100 mol), anhydrous K_2CO_3 (1.38 g, 0.0100 mol) and (0.0120 mol) of 2-chloro-1-[4-(2-substitutedphenyl)-piperazin-1-yl]-ethanone (**IIIa–c**) in (30 mL) dry acetone for 12 h. The reaction was then filtered, washed with ethanol. The filtrate was concentrated and the formed precipitate was collected, dried and crystallized from methanol/ethyl acetate mixture to give pure solids of **IVa–c**.

*4.2.5.1. 6-Methyl-2-[2-oxo-2-(4-phenylpiperazin-1-yl)-ethylamino]-4,5,7-tetrahydrothieno[2,3-c]pyridine-3-carboxylic acid amide (**IVa**): Yield.* 63%; m.p.: 77–80 °C; **^{1}H NMR** (500 MHz, DMSO): δ 2.29 (s, 3H, CH_3—N), δ 2.7 (t, *J* = 5.2 Hz, 2H, $\underline{CH_2}$—N of pyridine), δ 2.59 (t, *J* = 5.2 Hz, 2H, $\underline{CH_2}CH_2$—N of pyridine), δ 3.6 (s, 2H, $\underline{CH_2}$—N of pyridine), δ 3.5 (t, *J* = 5.2 Hz, 4H, 2$\underline{CH_2}$—N of piperazine), δ 3.8 (t, *J* = 5.1 Hz, 4H, 2$\underline{CH_2}$—N of piperazine), δ 4.09 (s, 2H, NH—$\underline{CH_2}$—CO), δ 6.6–7.1 (m, 5H, Ar); **FT-IR** ($\tilde{V}$ max, cm^{-1}): 1597&1635 (2 C=O), 2819–2937 (CH aliphatic), 3026–3055 (CH Ar), 3388 (NH amide); MS (M.Wt.: 413): *m/z* 413 (M+, 100%). Anal. Calcd for $C_{21}H_{27}N_5O_2S$: C, 60.99; H, 6.58; N, 16.94 Found: C, 61.25; H, 6.53; N, 17.32.

*4.2.5.2. 2-{2-[4-(2-Methoxyphenyl)-piperazin-1-yl]-2-oxo-ethylamino}-6-methyl-4,5,7-tetrahydrothieno[2,3-c]pyridine-3-carboxylic acid amide (**IVb**).* **Yield:** 91%; m.p.: 94–95 °C; **^{1}H NMR** (300 MHz, DMSO): δ 2.28 (s, 3H, CH_3—N), δ 3.0 (t, *J* = 5.8 Hz, 2H, $\underline{CH_2}$—N of pyridine), δ 2.79 (t, *J* = 5.8 Hz, 2H, $\underline{CH_2}CH_2$—N of pyridine), δ 3.69 (s, 2H, $\underline{CH_2}$—N of pyridine), δ 3.47 (t, 4H, 2$\underline{CH_2}$—N of piperazine), δ 3.6 (t, 4H, 2$\underline{CH_2}$—N of piperazine), δ 4.11 (s, 2H, NH—$\underline{CH_2}$—CO), δ 3.78 (s, 3H, Ph-$\underline{OCH_3}$), δ 6.7–7.1 (m, 4H, Ar); **FT-IR** ($\tilde{V}$ max, cm^{-1}): 1641&1656 (2C=O), 2831–2997 (CH, aliphatic), 3061 (CH Ar), 3388 (NH); MS (M.Wt.: 443): *m/z* 441 (M+, 100%). Anal. Calcd for $C_{22}H_{29}N_5O_3S$: C, 59.57; H, 6.59; N, 15.79 Found: C, 59.91; H, 6.45; N, 16.11.

*4.2.5.3. 2-{2-[4-(2-Flourophenyl)-piperazin-1-yl]-2-oxo-ethylamino}-6-methyl-4,5,7-tetrahydrothieno[2,3-c]pyridine-3-carboxylic acid amide (**IVc**).* **Yield:** 67%; m.p.: 85–87 °C; **^{1}H NMR** (300 MHz, DMSO): δ 2.26 (s, 3H, CH_3—N), δ 2.93 (t, *J* = 5.9 Hz, 2H, $\underline{CH_2}$—N of pyridine), δ 2.61 (t, *J* = 5.9 Hz, 2H, $\underline{CH_2}CH_2$—N of pyridine), 3.68 (s, 2H, $\underline{CH_2}$—N of pyridine), δ 3.31 (t, 4H, 2$\underline{CH_2}$—N of piperazine), δ 3.69 (t, 4H, 2$\underline{CH_2}$—N of piperazine), δ 4.10 (s, 2H, NH—$\underline{CH_2}$—CO), δ 6.6–6.88 (m, 4H, Ar); **FT-IR** ($\tilde{V}$ max, cm^{-1}): 1629&1641 (2C=O), 2829–2945 (CH, aliphatic), 3039–3066 (CH, Ar), 3396 (NH); MS (M.Wt.: 431): *m/z* 431(M+, 100%). Anal. Calcd for $C_{21}H_{26}FN_5O_2S$: C, 58.45; H, 6.07; N, 16.23 Found: C, 58.63; H, 6.15; N, 16.70.

*4.2.5.4. 2-{3-[4-(2-or3-Substitutedphenyl)-piperazin-1-yl]-propylamino}-6-methyl-4,5,7-tetrahydrothieno[2,3-c]pyridine-3-carboxylic acid amide derivatives (**VIa–d**): General procedures.* To a stirred solution of ***II*** (2.11 g, 0.0100 mol) and anhydrous K_2CO_3 (4.14 g, 0.0300 mol) in (30 mL) dry acetone, (0.0120 mol) of 1-(3-chloropropyl)-4-(2-substituted-phenyl)-piperazines (***Va–c***) were added for compounds ***VIa–c*** or (3.7 g, 0.0120 mol) of 1-(3-chloropropyl)-4-(3-chlorophenyl)-piperazine was added for compound ***VId***. Stirring and reflux were continued for 12 h. The reaction mixture was then filtered while hot, washed with ethanol and the filtrate was concentrated under vacuum. The solid formed was filtered and crystallized from methanol/ethyl acetate mixture to yield the titled compounds.

*4.2.5.5. 6-Methyl-2-[3-(4-pheny-piperazin-1-yl)-propylamino]-4,5,7-tetrahydrothieno[2,3-c]pyridine-3-carboxylic acid amide (**VIa**).* **Yield:** 85%; m.p.: 73–74 °C; **^{1}H NMR** (500 MHz, DMSO): δ 3.04 (t, *J* = 5.2 Hz, 2H, N—$\underline{CH_2}$—CH_2—CH_2), δ 1.9 (m, *J* = 5.2 Hz, 2H, N—CH_2—$\underline{CH_2}$—CH_2), δ 2.34 (t, *J* = 5.2 Hz, 2H, N—CH_2—CH_2—$\underline{CH_2}$), δ 2.36 (s, 3H, CH_3—N), δ 2.84 (t, *J* = 5.7 Hz, 2H, C$\underline{H_2}$—N of pyridine), δ 2.73 (t, *J* = 5.7 Hz, 2H, $\underline{CH_2}$—CH_2—N of pyridine), δ 3.68 (s, 2H, $\underline{CH_2}$—N of pyridine), δ 2.71 (t, 4H, 2C$\underline{H_2}$—N of piperazine), δ 3.53 (t, 4H, 2C$\underline{H_2}$—N of piperazine), δ 6.63–7.01 (m, 5H, Ar); **FT-IR** ($\tilde{V}$, max, cm^{-1}): 1635&1650 (C=O amide), 2823–2924 (CH aliphatic), 3032–3062 (CH aromatic), 3390–3450 (NH_2 amide); MS: 413(M^+, 100%); Anal. Calcld for $C_{22}H_{31}N_5OS$: C, 63.89; H, 7.56; N, 16.93 Found C, 64.08; H, 7.63; N, 17.14.

*4.2.5.6. 2-{3-[4-(2-Methoxyphenyl)-piperazin-1-yl]-propylamino}-6-methyl-4,5,7-tetrahydrothieno[2,3-c]pyridine-3-carboxylic acid amide **VIb**.* **Yield:** 83%; m.p.: 98–100 °C; **^{1}H NMR** (500 MHz, $CDCl_3$): δ 3.08 (t, *J* = 5.4 Hz, 2H, N—$\underline{CH_2}$—CH_2—CH_2), δ 1.26 (m, *J* = 5.4 Hz, 2H, N—CH_2—$\underline{CH_2}$—CH_2), δ 2.47 (t, *J* = 5.4 Hz, 2H, N—CH_2—CH_2—$\underline{CH_2}$), δ 2.17 (s, 3H, CH_3—N), δ 2.78 (t, *J* = 5.9 Hz, 2H, C$\underline{H_2}$—N of pyridine), δ 2.74 (t, *J* = 5.9 Hz, 2H, $\underline{CH_2}$—CH_2—N of pyridine), δ 3.68 (s, 2H, C$\underline{H_2}$—N of pyridine), δ 2.72 (t, 4H, 2C$\underline{H_2}$—N of piperazine), δ 3.38 (t, 4H, 2C$\underline{H_2}$—N of piperazine), δ 3.85 (s, 3H, Ph-$\underline{OCH_3}$), δ 6.74–6.90 (m, 4H, Ar); **FT-IR** ($\tilde{V}$ max, cm^{-1}): 1650 (C=O amide), 2831–2927 (CH aliphatic), 3032–3066 (CH Ar), 3394–3417 (NH, NH_2); MS: (M.Wt.: 431): *m/z* 443(M+, 100%). Anal. Calcd for $C_{23}H_{33}N_5O_2S$: C, 62.27; H, 7.50; N, 15.79 Found C, 62.41; H, 7.13; N, 16.02.

*4.2.5.7. 2-{3-[4-(2-Flourophenyl)-piperazin-1-yl]-propylamino}-6-methyl-4,5,7-tetrahydrothieno[2,3-c]pyridine-3-carboxylic acid amide (**VIc**).* **Yield:** 59%; m.p.: 67–68 °C; **^{1}H NMR** (500 MHz, $CDCl_3$): δ 3.35 (t, *J* = 5.3 Hz, 2H, N—$\underline{CH_2}$—CH_2—CH_2), δ 1.96 (m, *J* = 5.3 Hz, 2H, N—CH_2—$\underline{CH_2}$—CH_2), δ 2.48 (t, *J* = 5.3 Hz, 2H, N—CH_2—CH_2—$\underline{CH_2}$), δ 2.17 (s, 3H, CH_3—N), δ 2.78 (t, *J* = 6.6 Hz, 2H, C$\underline{H_2}$—N of pyridine), δ 2.72 (t, *J* = 6.6 Hz, 2H, $\underline{CH_2}$—CH_2—N of pyridine), δ 3.74 (s, 2H, C$\underline{H_2}$—N of pyridine), δ 2.64 (t, 4H, 2C$\underline{H_2}$—N of piperazine), δ 3.57 (t, 4H, 2C$\underline{H_2}$—N of piperazine), δ 6.61–7.08 (m, 4H, Ar); **FT-IR** ($\tilde{V}$ max, cm^{-1}): 1650 (C=O amide), 2831–2927 (CH aliphatic), 3032–3066 (CH Ar), 3394–3417 (NH, NH_2); MS (M.Wt.: 431): *m/z* 443 (M+, 100%). Anal. Calcd for $C_{22}H_{30}FN_5OS$: C, 61.23; H, 7.01; N, 16.23 Found C, 61.35; H, 7.12; N, 16.58.

*4.2.5.8. 2-{3-[4-(3-Chlorophenyl)-piperazin-1-yl]-propylamino}-6-methyl-4,5,7-tetrahydrothieno[2,3-c]pyridine-3-carboxylic acid amide (**VId**).* **Yield:** 40%); m.p.: 110–113 °C; **^{1}H NMR** (500 MHz, $CDCl_3$): δ 3.21 (t, *J* = 5.2 Hz, 2H, N—$\underline{CH_2}$—CH_2—CH_2), δ 1.25 (m, *J* = 5.2 Hz, 2H, N—CH_2—$\underline{CH_2}$—CH_2), δ 2.47 (t, *J* = 5 Hz, 2H, N—CH_2—CH_2—$\underline{CH_2}$), δ 2.15 (s, 3H, CH_3—N), δ 2.93 (t, *J* = 5.6 Hz, 2H, C$\underline{H_2}$—N of pyridine), δ 2.81 (t, *J* = 5.4 Hz, 2H, $\underline{CH_2}$—CH_2—N of pyridine), δ 3.65 (s, 2H, C$\underline{H_2}$—N of pyridine), δ 2.62 (t, 4H, 2C$\underline{H_2}$—N of piperazine), δ 3.69 (t, 4H, 2C$\underline{H_2}$—N of piperazine), δ 6.50–7.02 (m, 4H, Ar); MS (M.Wt.: 447): *m/z* 447 (M+, 100%), 449 (M + 2, 24.5%); Anal. Calcd for $C_{22}H_{30}ClN_5OS$: C, 58.98; H, 6.75; N, 15.63 Found C, 58.68; H, 6.52; N, 15.97.

*4.2.5.9. 2-{2-[4-(2-Substitutedphenyl)-piperazin-1-yl]-acetylamino}-6-methyl-4,5,7-tetrahydrothieno[2,3-c]pyridine-3-carboxylic acid amide derivatives (**VIIIa–c**): General procedures.* The titled compounds ***VIIIa–c*** were prepared by refluxing compound ***VII*** (2.87 g, 0.0100 mol) with different (1or 2-substitutedphenyl)-piperazines (0.0120 mol) and anhydrous K_2CO_3 (1.38 g, 0.0100 mol) in DMF (20 mL) for 12 h. The reaction was diluted with iced cold water. The yellow solid formed was filtered, dried and crystallized from absolute ethanol.

*4.2.5.10. 6-Methyl-2-[2-(4-phenylpiperazin-1-yl)-acetylamino]-4,5,7-tetrahydrothieno[2,3-c]pyridine-3-carboxylic acid amide (**VIIIa**).* **Yield:** 68%; m.p.: 200 °C; **^{1}H NMR (300** MHz, **$CDCl_3$):** δ 2.55 (s, 3H, C$\underline{H_3}$—N), δ 2.85 (t, *J* = 5.9 Hz, 2H, C$\underline{H_2}$—N of pyridine), δ 2.87 (t, *J* = 5.9 Hz, 2H, $\underline{CH_2}$—CH_2—N of pyridine), δ 3.65 (s, 2H, C$\underline{H_2}$—N of pyridine), δ 2.87 (t, 4H, 2C$\underline{H_2}$—N of piperazine), δ 3.42 (t, 4H, 2C$\underline{H_2}$—N of piperazine), δ 6.60–7.01 (m, 5H, Ar) δ 3.30 (s, 2H, CO—$\underline{CH_2}$—N); **FT-IR (**$\tilde{V}$ max, cm^{-1}**):** 1674&1645 (C=O), 2945–2819 (CH aliphatic), 3157–3024 (CH Ar), 3502–3307 (NH amide); **MS** (M.Wt.: 413): *m/z* 414 (M+, 100%); Anal. Calcd for $C_{21}H_{27}N_5O_2S$: C, 60.99; H, 6.58; N, 16.94 Found C, 61.14; H, 6.83; N, 17.32.

*4.2.5.11. 2-{2-[4-(2-Methoxyphenyl)-piperazin-1-yl]-acetylamino}-6-methyl-4,5,7-tetrahydrothieno[2,3-c]pyridine-3-carboxylic acid amide (**VIIIb**).* **Yield:** 64%; m.p.: 111–112 °C; **^{1}H NMR** (300 MHz, $CDCl_3$): δ 2.38 (s, 3H, C$\underline{H_3}$—N), δ 2.78 (t, *J* = 5.9 Hz, 2H, C$\underline{H_2}$—N of

pyridine), δ 2.74 (t, *J* = 5.9 Hz, 2H, $\underline{CH_2}$—CH_2—N of pyridine), δ 3.54 (s, 2H, $C\underline{H_2}$—N of pyridine), δ 2.48 (t, 4H, $2C\underline{H_2}$—N of piperazine), δ 3.18 (t, 4H, $2C\underline{H_2}$—N of piperazine), δ 6.70–6.88 (m, 4H, Ar) δ 2.95 (s, 2H, CO—$\underline{CH_2}$—N); δ 3.86 (s, 3H, Ph-$\underline{OCH_3}$); **FT-IR** ($\tilde{V}$ max, cm^{-1}): 1654 (C=O), 2819–2993 (CH aliphatic), 3061–3157 (CH Ar), 3427–3498 (NH amide); MS: (M.Wt.: 443): *m/z* 443(M+, 100%); Anal. Calcd for $C_{22}H_{29}N_5O_3S$: C, 59.57; H, 6.59; N, 15.79 Found C, 59.78; H, 6.86; N, 16.13.

*4.2.5.12. 2-{2-[4-(2-Fluorophenyl)-piperazin-1-yl]-acetylamino}-6-methyl-4,5,7-tetrahydrothieno[2,3-c]pyridine-3-carboxylic acid amide (**VIIIc**).* **Yield:** 67%; m.p.: 185 °C; **^{1}H NMR** (300 MHz, $CDCl_3$): δ 2.60 (s, 3H, $C\underline{H_3}$—N), δ 2.69 (t, 2H, $C\underline{H_2}$—N of pyridine), δ 2.73 (t, *J* = 5.9 Hz, 2H, $\underline{CH_2}$—CH_2—N of pyridine), δ 3.78 (s, 2H, $C\underline{H_2}$—N of pyridine), δ 2.87 (t, 4H, $2C\underline{H_2}$—N of piperazine), δ 3.31 (t, 4H, $2C\underline{H_2}$—N of piperazine), δ 6.62–7.08 (m, 4H, Ar) δ 3.31 (s, 2H, CO—$\underline{CH_2}$—N); **FT-IR** ($\tilde{V}$ max, cm^{-1}): 1674&1647 (C=O), 2991–2825 (CH aliphatic), 3159–3034 (CH Ar), 3506–3307 (NH amide); MS (M.Wt.: 431): *m/z* 431 (M^+, 100%); Anal. Calcd for $C_{21}H_{26}FN_5O_2S$: C, 58.45; H, 6.07; N, 16.23 Found C, 58.57; H, 6.14; N, 16.47.

*4.2.5.13. 7-Methyl-2-[(2-oxo-2-(4-(2-substitutedphenyl)piperazin-1-yl)ethyl)thio]-5,6,7,8-tetrahydropyrido[4′,3′:4,5]-thieno[2,3-d]-pyrimidin-4-one derivatives (**Xa–c**): General procedures.* Compounds ***Xa–c*** were prepared by refluxing ***IX*** (2.53 g, 0.0100 mol) with KOH (0.56 g, 0.0100 mol) in absolute ethanol (32 mL) for 30 min. After which the phenylpiperazines ***IIIa–c*** (0.0120 mol) were added. Stirring and reflux were continued for 20 h. The reaction mixture was filtered while hot, washed with ethanol and concentrated under vacuum. The formed solid was filtered and crystallized from absolute ethanol.

*4.2.5.14. 7-Methyl-2-[(2-oxo-2-(4-(phenyl)piperazin-1-yl)ethyl)thio]-5,6,7,8-tetrahydropyrido[4′,3′:4,5]-thieno[2,3-d]-pyrimidin-4-one (**Xa**).* **Yield:** 70%; m.p.: 128–129 °C; **^{1}H NMR** (300 MHz, DMSO): δ 2.30 (s, 3H, $C\underline{H_3}$—N), δ 2.77 (t, *J* = 5.8 Hz, 2H, $C\underline{H_2}$—N of pyridine), δ 2.61 (t, *J* = 5.8 Hz, 2H, $\underline{CH_2}$—CH_2—N of pyridine), δ 3.78 (s, 2H, $C\underline{H_2}$—N of pyridine), δ 3.31 (t, 4H, $2C\underline{H_2}$—N of piperazine), δ 3.78 (t, 4H, $2C\underline{H_2}$—N of piperazine), δ 6.50–7.02 (m, 5H, Ar), δ 3.77 (s, 2H, S—$\underline{CH_2}$—CO); **FT-IR** ($\tilde{V}$ max, cm^{-1}): 1631&1597 (C=O), 2821–2916 (CH aliphatic), 3001–3107 (CH aromatic), 3439 (NH amide); MS (M.Wt.: 455): *m/z* 455 (M+, 100%); Anal. Calcd for $C_{22}H_{25}N_5O_2S_2$: C, 58.00; H, 5.53; N, 15.37 Found C, 58.4; H, 5.61; N, 15.56.

*4.2.5.15. 7-Methyl-2-[(2-oxo-2-(4-(2-Methoxyphenyl)piperazin-1-yl)ethyl)thio]-5,6,7,8-tetrahydropyrido[4′,3′:4,5]-thieno[2,3-d]-pyrimidin-4-one (**Xb**).* **Yield:** 57%; m.p.: 140–142 °C; **^{1}H NMR** (300 MHz, DMSO):): δ 2.28 (s, 3H, $C\underline{H_3}$—N), δ 2.92 (t, *J* = 5.7 Hz, 2H, $C\underline{H_2}$—N of pyridine), δ 2.74 (t, *J* = 5.7 Hz, 2H, $\underline{CH_2}$—CH_2—N of pyridine), δ 3.72 (s, 2H, $C\underline{H_2}$—N of pyridine), δ 3.54 (t, 4H, $2C\underline{H_2}$—N of piperazine), δ 3.64 (t, 4H, $2C\underline{H_2}$—N of piperazine), δ 6.62–7.01 (m, 4H, Ar), δ 3.97 (s, 2H, S—$\underline{CH_2}$—CO), δ 3.84 (s, 3H, Ph-$\underline{OCH_3}$); **FT-IR** ($\tilde{V}$ max, cm^{-1}): 1639 (C=O), 2827–2908 (CH aliphatic), 3421 (NH amide); MS (M.Wt.: 485): *m/z* 485 (M+, 100%); Anal. Calcd for $C_{23}H_{27}N_5O_3S_2$: C, 56.88; H, 5.60; N, 14.42 Found C, 57.02; H, 5.62; N, 14.83.

*4.2.5.16. 7-Methyl-2-[(2-oxo-2-(4-(2-flourophenyl)piperazin-1-yl)ethyl)thio]-5,6,7,8-tetrahydropyrido[4′,3′:4,5]-thieno[2,3-d]-pyrimidin-4-ones (**Xc**).* **Yield:** 53%; m.p.: 110 °C; **^{1}H NMR** (300 MHz, DMSO): δ 2.3 (s, 3H, $C\underline{H_3}$—N), δ 3.03 (t, 2H, $C\underline{H_2}$—N of pyridine), δ 2.73 (t, *J* = 5.7 Hz, 2H, $\underline{CH_2}$—CH_2—N of pyridine), δ 3.62 (s, 2H, $C\underline{H_2}$—N of pyridine), δ 3.66 (t, 4H, $2C\underline{H_2}$—N of piperazine), δ 3.71 (t, 4H, $2C\underline{H_2}$—N of piperazine), δ 6.70–7.02 (m, 4H, Ar), δ 4.14 (s, 2H, S—$\underline{CH_2}$—CO); **FT-IR** ($\tilde{V}$ max, cm^{-1}): 1631&1612 (2 C=O), 2825–2995 (CH aliphatic), 3385 (NH amide); MS (M.Wt.: 473): *m/z* 473 (M^+, 100%); Anal. Calcd for $C_{22}H_{24}FN_5O_2S_2$: C, 55.79; H, 5.11; N, 14.79; Found C, 55.86; H, 5.19; N, 15.18.

*4.2.5.17. 7-Methyl-2-[[3-[4-(2or3-substitutedphenyl)-1-piperazinyl]propyl]thio]-3,5,6,8-tetrahydropyrido[4′,3′:4,5]thieno[2,3-d] pyrimidin-4-onederivatives (**XIa–d**): General procedures.* Compounds ***XIa–d*** were prepared by refluxing ***IX*** (2.53 g, 0.0100 mol) with KOH (0.56 g, 0.0100 mol) in absolute ethanol (32 mL) for 30 min, after which (0.0120 mol) of 1-(3-chloropropyl)-4-(2-substitutedphenyl)-piperazines (***Va-c***) were added for compounds ***XIa–c*** or (3.7 g, 0.0120 mol) of 1-(3-chloropropyl)-4-(3-chlorophenyl)-piperazine for compound ***XId***. The solution was refluxed for 20 h. The reaction mixture was filtered while hot, washed with ethanol and concentrated under vacuum. The formed solid was filtered and crystallized from absolute ethanol.

*4.2.5.18. 7-Methyl-2-[[3-[4-(phenyl)-1-piperazinyl] propyl] thio]-5,6,7,8-pyrido[4′,3′:4,5]thieno[2,3-d]pyrimidin-4-one (**XIa**).* **Yield:** 64%; m.p.: 95–97 °C; **^{1}H NMR** (300 MHz, DMSO): δ 3.07 (t, *J* = 4.9 Hz, 2H, S—$\underline{CH_2}$—CH_2—CH_2), δ 1.87 (m, *J* = 4.9 Hz, 2H, S—CH_2—$\underline{CH_2}$—CH_2), δ 2.51 (t, *J* = 5.2 Hz, 2H, S—CH_2—CH_2—$\underline{CH_2}$), δ 2.34 (s, 3H, CH_3—N), δ 2.81 (t, 2H, $C\underline{H_2}$—N of pyridine), δ 2.74 (t, 2H, $\underline{CH_2}$—CH_2—N of pyridine), δ 3.48 (s, 2H, $C\underline{H_2}$—N of pyridine), δ 2.82 (t, 4H, $2C\underline{H_2}$—N of piperazine), δ 3.32 (t, 4H, $2C\underline{H_2}$—N of piperazine), δ 6.69–7.06 (m, 5H, Ar); **FT-IR** ($\tilde{V}$ max, cm^{-1}): 1647 (C=O), 2796–2964 (CH aliphatic), 3037–3165 (CH Ar), 3508 (NH amide); MS (M.Wt.: 455): *m/z* 455 (M+, 100%); Anal. Calcd for $C_{23}H_{29}N_5OS_2$: C, 60.63; H, 6.42; N, 15.37 Found C, 61.11; H, 6.38; N, 15.61.

*4.2.5.19. 7-Methyl-2-[[3-[4-(2-methoxyphenyl)-1-piperazinyl]propyl]thio]-5,6,7,8-pyrido[4′,3′:4,5]thieno[2,3-d]pyrimidin-4(3H)-one (**XIb**).* **Yield:** 55%; m.p.: 114 °C; **^{1}H NMR** (500 MHz, DMSO): δ 3.15 (t, *J* = 5.6 Hz, 2H, S—$\underline{CH_2}$—CH_2—CH_2), δ 2.06 (m, *J* = 5.6 Hz, 2H, S—CH_2—$\underline{CH_2}$—CH_2), δ 2.38 (t, *J* = 5.6 Hz, 2H, S—CH_2—CH_2—$\underline{CH_2}$), δ 2.27 (s, 3H, CH_3—N), δ 2.90 (t, *J* = 5.4 Hz, 2H, $C\underline{H_2}$—N of pyridine), δ 2.75 (t, *J* = 5.4 Hz, 2H, $\underline{CH_2}$—CH_2—N of pyridine), δ 3.73 (s, 2H, $C\underline{H_2}$—N of pyridine), δ 2.83 (t, 4H, $2C\underline{H_2}$—N of piperazine), δ 3.32 (t, 4H, $2C\underline{H_2}$—N of piperazine), δ 6.73–6.89 (m, 4H, Ar), δ 3.70 (s, 3H, Ph-$\underline{OCH_3}$); **FT-IR** ($\tilde{V}$ max, cm^{-1}): 1624 (C=O), 2812–2939 (CH-aliphatic), 3090–3167 (CH—Ar), 3425 (NH—); MS (M.Wt.: 485): *m/z* 485(M+, 100%); Anal. Calcd for $C_{24}H_{31}N_5O_2S_2$: C, 59.35; H, 6.43; N, 14.42 Found C, 59.32; H, 6.52; N, 14.81.

*4.2.5.20. 7-Methyl-2-[[3-[4-(2-flouro-phenyl)-1-piperazinyl]propyl] thio]-5,6,7,8-pyrido[4′,3′:4,5]thieno[2,3-d]pyrimidin-4(3H)-one (**XIc**).* **Yield:** 77%; m.p.: 116–117 °C; **^{1}H NMR** (500 MHz, DMSO): δ 2.98 (t, *J* = 6.9 Hz, 2H, S—$\underline{CH_2}$—CH_2—CH_2), δ 1.81 (m, *J* = 6.9 Hz, 2H, S—CH_2—$\underline{CH_2}$—CH_2), δ 2.46 (t, *J* = 6.9 Hz, 2H, S—CH_2—CH_2—$\underline{CH_2}$), δ 2.29 (s, 3H, CH_3—N), δ 2.94 (t, *J* = 5.9 Hz, 2H, $C\underline{H_2}$—N of pyridine), δ 2.74 (t, *J* = 5.9 Hz, 2H, $\underline{CH_2}$—CH_2—N of pyridine), δ 3.76 (s, 2H, $C\underline{H_2}$—N of pyridine), δ 2.78 (t, 4H, $2C\underline{H_2}$—N of piperazine), δ 3.56 (t, 4H, $2C\underline{H_2}$—N of piperazine), δ 6.63–6.99 (m, 4H, Ar); **FT-IR** ($\tilde{V}$ max, cm^{-1}): 1685 (C=O), 2812–2943 (CH aliphatic), 3039–3062 (CH Ar), 3410 (NH); MS (M.Wt.: 473), *m/z*: (473, M+, 100%); Anal. Cacld for $C_{23}H_{28}FN_5OS_2$: C, 58.33; H, 5.96; N, 14.79 Found C, 58.68; H, 5.94; N, 15.13.

*4.2.5.21. 7-Methyl-2-[[3-[4-(3-chlorophenyl)-1-piperazinyl]propyl]thio]-3,5,6,8-tetrahydropyrido[4′,3′:4,5]thieno[2,3-d]pyrimidin-4-one (**XId**).* **Yield:** 63%; m.p.: 122 °C; **^{1}H NMR** (300 MHz, $CDCl_3$): δ 3.06 (t, *J* = 5.4 Hz, 2H, S—$\underline{CH_2}$—CH_2—CH_2), δ 1.96 (m, *J* = 5.4 Hz, 2H, S—CH_2—$\underline{CH_2}$—CH_2), δ 2.52 (t, *J* = 5.4 Hz, 2H, S—CH_2—CH_2—$\underline{CH_2}$), δ 2.46 (s, 3H, CH_3—N), δ 2.99 (t, Hz, 2H, $C\underline{H_2}$—N of pyridine), δ 2.67 (t, 2H, $\underline{CH_2}$—CH_2—N of pyridine), δ 3.74 (s, 2H, $C\underline{H_2}$—N of pyridine), δ 2.54 (t, 4H, $2C\underline{H_2}$—N of piperazine), δ 3.13 (t, 4H, $2C\underline{H_2}$—N of piperazine), δ 6.52–7.02 (m, 4H, Ar); **FT-IR** ($\tilde{V}$ max, cm^{-1}): 1697

(C=O), 2787–2940 (CH aliphatic), 3388 (NH amide); MS: (M.Wt.: 490), *m/z*: 489 (M+, 100%), 491 (M+2, 41%); Anal. Calcld for $C_{23}H_{28}ClN_5OS_2$: C, 56.37; H, 5.76; N, 14.29 Found C, 56.39; H, 5.84; N, 14.53.

4.3. Pharmacology

Rats were euthanized by cervical dislocation and the thoracic aorta was carefully exposed and isolated. The isolated aorta was cut into rings (3–5 mm width) and each ring was then vertically mounted between two stainless steel hooks passed through its lumen. The lower hook was fixed between two plates, while the upper one was attached to a force displacement transducer (Model no. MLT0201, Panlab, Spain) connected to an amplifier (PowerLab, AdInstruments Pty. Ltd.) which is connected to a computer. The Chart for windows (v 3.4) software was used to record and elaborate data.

The isolated aortic ring was mounted in 10 ml water jacketed automatic multi-chamber organ bath system (Model no. ML870B6/C, Panlab, Spain). The organ bath contained Krebs' solution of the following composition (g/l): NaCl 6.9, KCl 0.35, KH_2PO_4 0.16, $MgSO_4{\cdot}7H_2O$ 0.3, $CaCl_2{\cdot}2H_2O$ 0.37, $NaHCO_3$ 2.1 and glucose 1.05. The organ bath solution was continuously aerated with carbogen (a mixture of 95% O_2 and 5% CO_2) and its temperature was kept at 37 °C. The preparation was allowed to equilibrate for about 120 min under a resting tension of 2 g during that time any change in the resting tension was readjusted. The aortic ring was contracted by norepinephrine ($10\ M^{-6}$).

Pre-exposure of the aortic ring to α-blocker is supposed to suppress norepinephrine induced aortic contraction. Percent change in aortic tension was calculated for compounds under investigation ($10\ M^{-6}$) and compared to standard α-blocker, prazosin (***1***) ($10\ M^{-6}$). Change in aortic tension was recorded and calculated over a period of one minute and average tension was used for calculation [24].

References

[1] A. Hirasawa, K. Shibata, K. Horie, Y. Takei, K. Obika, T. Tanaka, N. Muramoto, K. Takagaki, J. Yana, G. Tsujimoto, Cloning, functional expression and tissue distribution of human α_{1c}-adrenoceptor splice variants, FEBS Lett. 363 (1995) 256–260.

[2] J. Handzlik, D. Macia, M. Kubacka, S. Mogilski, B. Filipek, K. Stadnickad, K. Kieć-Kononowicz, Synthesis, α_1-adrenoceptor antagonist activity, and SAR study of novel arylpiperazine derivatives of phenytoin, Bioorg. Med. Chem. 16 (2008) 5982–5998.

[3] M. Rosini, M.L. Bolognesi, D. Giardinà, A. Minarini, V. Tumiatti, C. Melchiorre, Recent advances in alpha1-adrenoreceptor antagonists as pharmacological tools and therapeutic agents, Curr. Top. Med. Chem. 7 (2007) 147–162.

[4] G. Romeo, L. Materia, L. Salerno, F. Russo, K.P. Minneman, Novel antagonists for α1-adrenoreceptor subtypes, Exp. Opin. Ther. Patents 14 (2004) 619–637.

[5] S. Cotecchia, J. Recept., The α1-adrenergic receptors: diversity of signaling networks and regulation, Signal Transduct. 30 (2010) 410–419.

[6] J.B. Bremner, B. Coban, R. Grith, K.M. Groenewoud, B.F. Yates, Ligand design for $\alpha_1$adrenoceptor subtype selective antagonists, Bioorg. Med. Chem. 8 (2000) 201–214.

[7] R. Barbaro, L. Betti, M. Botta, F. Corelli, G. Giannaccini, L. Maccari, F. Manetti, G. Strappaghetti, S. Corsano, Synthesis, biological evaluation, and pharmacophore generation of new pyridazinone derivatives with affinity toward α_1- and α_2-adrenoceptors, J. Med. Chem. 44 (2001) 2118–2132.

[8] G.S. Hassan, Design and synthesis of some piperazinomethyl benzofuran derivatives and preliminary investigation of their hypotensive activity as α1 adrenoreceptor antagonists, Int. J. Pharm. Pharmaceut. Sci. 3 (2011) 441–449.

[9] I.J.A. MacDougall, R. Griffith, Selective pharmacophore design for α1-adrenoceptor subtypes, J. Mol. Graph. Model. 25 (2006) 146–157.

[10] J. Handzlik, H.H. Pertz, T. Görnemann, S. Jähnichen, K. Kieć-Kononowicz, Search for influence of spatial properties on affinity at α_1-adrenoceptor subtypes for phenylpiperazine derivatives of phenytoin, Bioorg. Med. Chem. Lett. 20 (2010) 6152–6156.

[11] M. Li, K. Tsaib, L. Xia, Pharmacophore identification of α_{1A}-adrenoceptor antagonists, Bioorg. Med. Chem. Lett. 15 (2005) 657–664.

[12] J. Handzlik, D. Macia, M. Kubacka, S. Mogilski, B. Filipek, K. Stadnickad, K. Kieć-Kononowicz, Synthesis, α_1-adrenoceptor antagonist activity, and SAR study of novel arylpiperazine derivatives of phenytoin, Bioorg. Med. Chem. 16 (2008) 5982–5998.

[13] K. Gewald, E. Schinke, H. Bottcher, 2-Amino-thiophene aus methylenaktiven Nitrilen, Carbonylverbindungen und Schwefel, Chem. Ber. 99 (1966) 94–100.

[14] L. Aurelio, C. Valant, H. Figler, B.L. Flynn, J. Linden, P.M. Sexton, A. Christopoulos, P.J. Scammells, 3- and 6-substituted 2-amino-4,5,6,7-tetrahydrothieno[2,3-c]pyridines as A_1 adenosine receptor allosteric modulators and antagonists, Bioorg. Med. Chem. 17 (2009) 7353–7361.

[15] J. Bourdais, Alkylation of piperazines in N,N-dimethylformamide, Bull. Soc. Chim. Fr. 8 (1968) 3246.

[16] M. Modica, M. Santagati, F. Russo, C. Selvaggini, A. Cagnotto, T. Mennini, High affinity and selectivity of [[(arylpiperazinyl) alkyl] thio] thieno[2,3-d] pyrimidinone derivatives for the 5-HT1A receptor. Synthesis and structure–affinity relationships, Eur. J. Med. Chem. 35 (2000) 677–689.

[17] A. Carrieri, A. Piergentili, F. Del Bello, M. Giannella, M. Pigini, A. Leonardi, F. Fanelli, W. Quaglia, Structure–activity relationships in 1,4-benzodioxan-related compounds. Novel α_1-adrenoreceptor antagonists related to openphendioxan: synthesis, biological evaluation, and α_1d computational study, Bioorg. Med. Chem. 18 (2010) 7065–7077.

[18] G. Romeo, L. Materia, M. Modica, V. Pittalà, L. Salerno, M.A. Siracusa, F. Manetti, M. Botta, K.P. Minneman, Novel 4-phenylpiperidine-2,6-dione derivatives. Ligands for α_1-adrenoceptor subtypes, Eur. J. Med. Chem. 46 (2011) 2676–2690.

[19] M.A. Ameen, S. Karsten, J. Liebscher, A convenient method for constructing novel tetrahydropyrido[4′,3′:4,5]thieno[2,3-d]pyrimidinones-carbohydrate and amino acid conjugates via copper(I)-catalyzed alkyne-azide 'Click Chemistry, Tetrahedron 66 (2010) 2141–2147.

[20] E.A. Bakhite, A.E. Abdel-Rahman, O.S. Mohamed, E.A. Thabet, Synthesis and reactions of new thienopyridines, pyridothienopyrimidines and pyridothienotriazines, Bull. Korean Chem. Soc. 23 (2002) 1709–1714.

[21] A.Y. Hassan, H.A. Mohamed, Synthesis and biological evaluation of thieno[2,3-c]pyridines and related heterocyclic systems, Asian J. Chem. 21 (2009) 3947–3961.

[22] S. Guccione, M. Modica, J. Longmore, D. Shaw, G.U. Barretta, A. Santagati, M. Santagati, F. Russo, Synthesis and NK-2 antagonist effect of 1,6-diphenyl-pyrazolo [3,4-d]-thiazolo[3,2-a]-4H-pyrimidin-4-one, Bioorg. Med. Chem. Lett. 6 (1996) 59–64.

[23] A. Santagati, J. Longmore, S. Guccione, T. Langer, E. Tonnel, M. Modica, M. Santagati, L.M. Scolaro, F. Russo, Building a model of interaction at the NK-2 receptors: polycondensed heterocycles containing the pyrimidoindole skeleton, Eur. J. Med. Chem. 32 (1998) 973–985.

[24] A.S. Girgis, N.S. Ismail, H. Farag, W.I. el-Eraky, D.O. Saleh, S.R. Tala, A.R. Katritzky, Regioselective synthesis and molecular modeling study of vasorelaxant active 7,9-dioxa-1,2-diaza-spiro[4.5]dec-2-ene-6,10-diones, Eur. J. Med. Chem. 45 (2010) 4229–4238.

[25] G.H. Kuo, C. Prouty, W.V. Murray, V. Pulito, L. Jolliffe, P. Cheung, S. Varga, M. Evangelisto, C. Shaw, Design, synthesis and biological evaluation of pyridine-phenylpiperazines: a novel series of potent and selective alpha1a-adrenergic receptor antagonist, Bioorg. Med. Chem. 8 (2000) 2263–2275.

[26] J.A. Garcia-Sainz, R. Villalobos-Molina, The elusive alpha (1D)-adrenoceptor: molecular and cellular characteristics and integrative roles, Eur. J. Pharmacol. 1–3 (2004) 113–120.